JOURNAL OF SOLID STATE CHEMISTRY **138,** 47–54 (1998)
ARTICLE NO. SC987753

Oxygen Release Behavior of $CeZrO_4$ Powders and Appearance of New Compounds κ and t*

Shinya Otsuka-Yao-Matsuo,[1] Takahisa Omata, Noriya Izu, and Haruo Kishimoto

Department of Materials Science and Processing, Graduate School of Engineering, Osaka University, Suita, Osaka 565-0871, Japan

Received August 25, 1997; in revised form January 8, 1998; accepted January 14, 1998

In order to clarify the chemical properties of the single phases, t′ and κ, in the CeO_2–ZrO_2 system, evolved-oxygen gas analyses (EGA) were performed by heating in a reducing gas and successive oxidations of the resulting pyrochlore phase in O_2 gas were carried out repeatedly. The rate of oxygen release was analyzed as a function of temperature and time. When the pyrochlore phase was oxidized at 873 K, the κ phase appeared. When the κ phase was annealed in O_2 gas at 1323 or 1423 K, a new tetragonal phase, t*, appeared, which released oxygen at the highest temperatures. The oxygen release behavior of the κ phase significantly changed, and was dependent on the history of the sample, specifically, whether it had experienced the t* phase. The oxygen release behavior of t′ depended on the temperature where the t′ had gained oxygen after losing a small amount of oxygen. Powder XRD and Raman scattering techniques have been applied to characterize the oxygen release behavior of these t′, t*, and κ phases. © 1998 Academic Press

1. INTRODUCTION

The phase diagram and phase transitions in the ZrO_2–CeO_2 system have been extensively reviewed by Yashima and Yoshimura (1); three types of tetragonal forms exist, t, t′, and t″. The t form appears on the ZrO_2-rich side of the equilibrium ZrO_2–CeO_2 phase diagram. The t″ form appearing in the CeO_2-rich side is a metastable phase. In the intermediate composition range of the ZrO_2–CeO_2 system, there exists no compound in the equilibrium phase diagram (2, 3) except for cubic solid solutions over 1823 K. However, once the cubic phase is cooled, a tetragonal t′ form (or phase) appears as a metastable single phase through a cation-diffusionless phase transition (4).

Because CeO_2–ZrO_2 powders release oxygen at relatively low temperatures, they are promising materials for sub-catalysts for automotive exhaust gases (5–8); the oxygen released can be used for the oxidation of harmful gases, i.e., transforming CO and HC to CO_2 and H_2O gases. In a previous study (9), the authors used t + CeO_2 two-phase mixtures coprecipitated from acid solution as starting samples and conducted an evolved-oxygen gas analysis (EGA) by heating them in a reducing gas with a constant P_{H_2O}/P_{H_2} gas ratio. By analysis of the amount of oxygen released, the phase diagram of the ZrO_2–CeO_2–$CeO_{1.5}$ system containing the t and CeO_2 phases was determined. When the sample was reduced to pyrochlore ($Ce_2Zr_2O_{7+y}$) and then oxidized at 873 K, it was found that the attained phases mainly consisted of a cubic phase with the composition range $x_{Ce}/(x_{Ce} + x_{Zr}) = 0.45$–$0.65$. This new cubic phase, previously called ϕ' (9), was renamed κ in this study. The κ phase released oxygen at a far lower temperature than did the t + CeO_2 two-phase mixtures; this property, which may be suitable for sub-catalysts, could be explained by a change in the phase diagram of the ZrO_2–CeO_2–$CeO_{1.5}$ system (9). Furthermore, it was experimentally demonstrated by the emf measurement of a galvanic cell that the thermodynamic stability of the κ phase is lower than that of t′ (10).

In the present study, we made a single phase of κ with composition $CeZrO_4$ using the pyrochlore ($Ce_2Zr_2O_{7+y}$), which was obtained by the reduction of the single phase of t′ ($CeZrO_4$) as a precursor. When the κ phase was annealed in O_2 gas at high temperatures, a new tetragonal phase appeared, which was named t* in this study. By repeating the reduction and oxidation of the t′ and t* (cyclic redox process), the κ phases exhibiting various oxygen release behaviors were obtained. In the present study, we tried to characterize the t′, t*, and various κ phases obtained through the cyclic redox process by means of EGA analysis, powder XRD, and Raman spectroscopy.

2. EXPERIMENTAL PRINCIPLE OF EGA ANALYSIS

Generally, a gas chromatography–mass spectrometry or mass thermobalance technique has been used to detect the oxygen released from a sample (8, 11). A closed-system potentiostatic technique employing a solid electrolyte, developed by one of the present authors (12–14), permits the measurements to be taken with much higher sensitivity and,

[1] To whom correspondence should be addressed.

0022-4596/98 $25.00

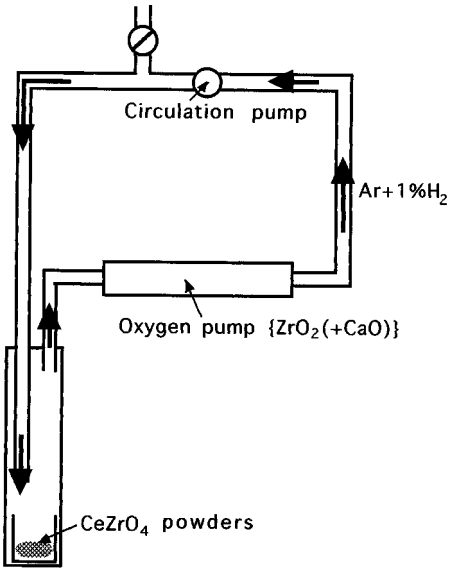

FIG. 1. Schematic description of the closed-system oxygen analyzer used for the evolved-oxygen gas analysis, (EGA).

therefore, with smaller amounts of samples than in conventional techniques. Measuring smaller amounts of samples creates a situation where the particles of the powders are rather isolated and the reaction proceeds homogeneously throughout the sample; this should lead to reproducible results, which are valuable for precise analysis.

The closed-system oxygen analyzer used in the present study is shown schematically in Fig. 1. It involves the electrochemical oxygen pump: Pt, air/$ZrO_2(+CaO)$ electrolyte/Ar, Pt. A $ZrO_2(+5$ mass% CaO) solid electrolyte tube with dimensions 21 mm o.d., 17 mm i.d., 500 mm long was supplied by Nippon Kagaku Togyo Co., Ltd. Platinum paste serving as an electrode was applied to the inside and outside surfaces of the tube, covering over 70 mm of the midsection. The sample powders were weighed, spread in an alumina crucible with a flat bottom (11 mm o.d., 9 mm i.d., 20 mm height), and then loaded into the reaction chamber of the oxygen analyzer. The electrochemical oxygen pump with four leads was heated to 1073 K. After the closed system was evacuated using a rotary pump, an $Ar + 1\%H_2$ gas mixture was introduced and then circulated at a flow rate of 900 $cm^3 \cdot min^{-1}$ in the direction indicated by the bold arrows in Fig. 1. The potentiostatic operation with four leads was carried out so that the emf, E, between the leads for emf measurements could be set to -1.3 V; the oxygen chemical potential at the solid electrolyte/Ar interface ($x = L$), $\mu(O_2)^L$, was maintained at a constant value. The corresponding oxygen partial pressure, $P(O_2)^L$, was evaluated to be $7.9 \times 10^{-25} \times 101325$ Pa using the equation (15):

$$E = (RT/4F)\ln\{P_{O_2}/(0.21 \times P^*)\}, \quad [1]$$

where R is the gas constant (8.31441 $J \cdot mol^{-1}$), T is the temperature (K), F is Faraday's constant (96,484.56 $C \cdot mol^{-1}$), P^* is 101,325 Pa.

Because the $P(O_2)^L$ value was very small, $Ar + H_2 + H_2O$ gas mixtures with a virtually constant $P(H_2O)/P(H_2)$ ratio, 4.2×10^{-4}, were circulated in the closed system. The electrical current passing through the electrochemical oxygen pump was converted to the corresponding voltage, and then transmitted to a personal computer at an interval of 0.425 s. The average value of 40 signals was obtained as the measured value of the current. Details of the experimental principles and techniques have been described in earlier papers (12, 16).

Because the oxygen in the closed system was electrochemically evacuated through the electrolyte, the $P(H_2O)/P(H_2)$ ratio of the circulating gas became constant, and the electric current, I, decreased to the base current, $I_\infty(t)$. As previously described (13, 14), the base current, $I_\infty(t)$, can be mainly attributed to the electrical components I_e^* and I'_{ion}; I_e^* is the electronic current, which is independent of time, and I'_{ion} is the ionic current due to the oxygen released from the electrolyte itself. A change in $I_\infty(t)$ with time can be expressed by a function, $I_\infty(t) = \exp\{-a(t+b)\} + c$ (9). After confirmation of the base current, $I_\infty(t)$, the evolved oxygen gas analysis was started by heating the sample chamber at a constant rate of $R = 2\ K \cdot min^{-1}$. When the oxygen is released from the sample into the system on heating, the oxygen chemical potential in the circulating gas, $\mu(O_2)^G$, becomes larger than $\mu(O_2)^L$. Because the oxygen is electrochemically pumped out of the system, the electric current, I, is increased from $I_\infty(t)$. Also, because the term, $\{I - I_\infty(t)\}$ is attributable to the ionic component, the amount of oxygen released or gained by the sample per second, J_O (O mol/s), is related to the current, I, by the equation:

$$J_O = \{I - I_\infty(t)\}/2F. \quad [2]$$

The total amount of oxygen, $N(O)$, in mol released by the sample in the reaction can be evaluated from the ionic charge, Q_{ion}, by integrating $\{I - I_\infty(t)\}$ over t:

$$N(O) = Q_{ion}/2F = (1/2F)\int\{I - I_\infty(t)\}\,dt$$
$$= \int J_O\,dt. \quad [3]$$

The closed system oxygen analyzer used in the present study was handmade; however, a similar type of oxygen analyzer is available from Toray Co., Ltd., Ohtsu City, Japan.

3. STARTING SAMPLES AND DETAILS OF EXPERIMENTAL TECHNIQUES

Starting Samples

CeO_2 (99.93 mass% purity) and ZrO_2 (99.97 mass% purity) powders were supplied from Mitsui Metal Co., Ltd.

Impurities in the CeO_2 powders were $Fe_2O_3 < 0.001$ mass%, $La_2O_3 < 0.03$ mass%, $Nd_2O_3 < 0.01$ mass%, $Pr_6O_{11} < 0.01$ mass%, and $Sm_2O_3 < 0.01$ mass%. Impurities in the ZrO_2 powders were $SiO_2 < 0.01$ mass%, $Fe_2O_3 < 0.001$ mass%, $TiO_2 < 0.005$ mass%, $Na_2O < 0.01$ mass%, and HfO_2 1.73 mass%. These were mixed in a mole ratio of 1:1 using a ball mill and pressed into a pellet under 270 MPa. The pellet was then sintered in air at 1823 K for 50 h to attain a cubic single phase; when it was cooled by cutting off the electric power, the phase transformed to t′($CeZrO_4$).

Experimental Procedures

Substances such as CO gas adsorbed in the system hinder precise EGA analysis because the CO may take oxygen from the sample to form CO_2 gas (16). Thus, the sample chamber containing an alumina crucible, which was placed in the closed-system oxygen analyzer, was heated once at 1323 K for 5 h by circulating pure O_2 gas. The system was then evacuated for a few minutes and cooled to room temperature.

The experimental procedures that follow this process are illustrated in Fig. 2. After the starting sample of t′ (about 35.5 mg) was loaded in the alumina crucible, it was heated at 1173 K in O_2 gas to remove substances adsorbed on the sample powders. In some of the experiments, the system was then evacuated for a few minutes at this temperature (preliminary vacuum treatment ①). After O_2 gas was introduced, the sample was cooled and annealed at 873 K for 5 h to control the oxygen content. In the other experiments, the system was evacuated not at 1173 K but at 373 K for a few minutes (preliminary vacuum treatment ②). After O_2 gas was introduced, the sample was heated and annealed at 873 K for 5 h to control the oxygen content. In the present study, the t′ phase annealed at 873 K for 5 h in pure O_2 gas at atmospheric pressure was regarded as the stoichiometric compound, $CeZrO_4$.

The samples of t′ were subjected to EGA analysis using the heating–cooling patterns ③ and ④ as shown in Fig. 2. After being cooled to 373 K in O_2 gas, the system was evacuated once, and then the Ar + 1%H_2 gas mixtures were introduced and circulated. In 10 h after the potentiostatic operation with four leads, the base current, $I_\infty(t)$, became small enough. Thus, an EGA analysis, i.e., the first heating-reduction run, was started by heating the sample at a rate of 2 K · min^{-1} to 1323 K. During the heating, the sample became a pyrochlore with oxygen being released.

During cooling from 1323 K to 873 K, the oxidation of the sample in the reducing gas was negligible. The system was evacuated and O_2 gas was introduced at 873 K, so that the sample could be oxidized again to its initial composition, $CeZrO_4$. After the sample was cooled to 373 K, the system was evacuated, and Ar + 1%H_2 gas was introduced

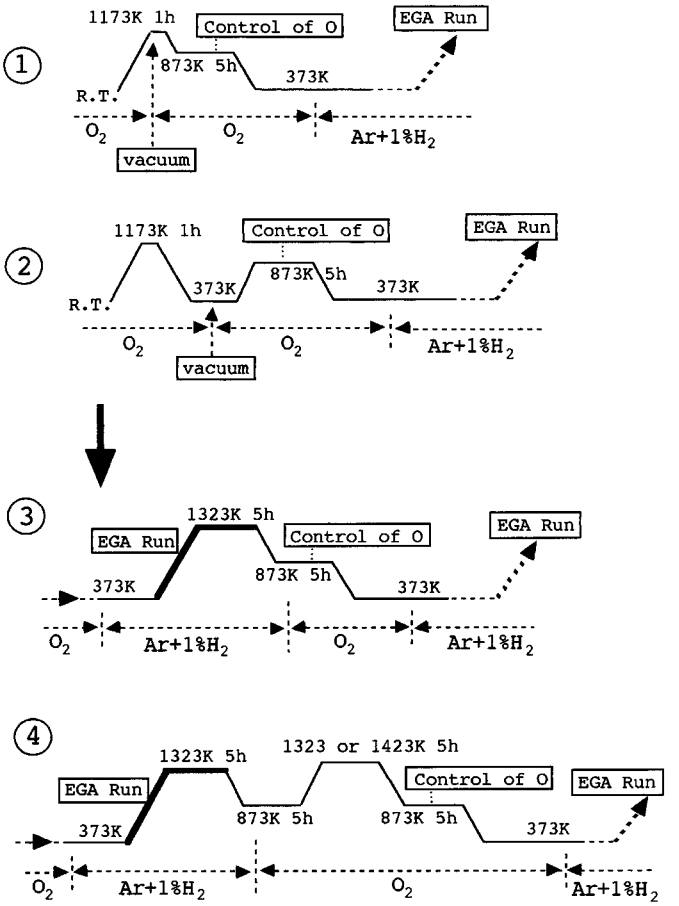

FIG. 2. Schematic description of the heating and cooling patterns used for the EGA analysis. ①: preliminary vacuum treatment at 1173 K; ②: preliminary vacuum treatment at 373 K; ③: heating-reduction run in a reducing gas; ④: heating-reduction run in a reducing gas and a successive annealing at 1323 or 1423 K in O_2 gas.

again. After the base current, $I_\infty(t)$ was confirmed, the second heating-reduction run was started. Several heating-reduction runs were repeated in a similar manner, i.e., using pattern ③, to check the reproducibility of the data.

In several runs, after the sample was oxidized at 873 K, i.e., the κ phase was formed, it was annealed at 1323 or 1423 K for 5 h, as shown by pattern ④ in Fig. 2. The sample, the oxygen content of which was controlled at 873 K, was subjected to successive heating-reduction runs.

The circulation pump was stopped at a preselected temperature in the heating-reduction runs, and the sample chamber with powders was quenched in ice and water. The sample phases were identified by X-ray diffraction using a diffractometer (Mac-Science Co., Ltd., MXP 18, Cu$K\alpha$ radiation), and furthermore, they were subjected to Raman scattering using a Jobin Yvon T64000 apparatus with an Ar laser (514.5 nm, Coherent Innova 300).

4. EXPERIMENTAL RESULTS

The amount of oxygen released from the sample, evaluated using Eq. [3], was well within the scattering of $\pm$ 2% for all of the heating-reduction runs. This means that the evacuation at 373 K immediately before the EGA run did not affect the oxygen content in the sample. The composition of the final pyrochlore phase was evaluated as $Ce_2Zr_2O_{7+y}$, with $y = 0.016$. Thus, a further discussion on the oxygen content of the samples will not be presented in this paper.

Figure 3 shows the J_o–T–t curves obtained when the starting phase t′ was subjected to the preliminary vacuum treatment ①. "a" and "A" in this figure indicate the history of the sample annealed in O_2 gas at 1323 K and 1423 K, respectively; for instance, the sample was annealed in O_2 gas at 1323 K after the third heating-reduction run, then the fourth run was undertaken, as illustrated in process ④ in Fig. 2. Furthermore, it was annealed in O_2 gas at 1423 K and 1323 K after the sixth and ninth runs, respectively. In Fig. 3, the symbol following the hyphen indicates the kind of phase ($CeZrO_4$) identified by XRD analysis and Raman spectroscopy. Lattice parameters of the t′, t*, κ, and pyrochlore, evaluated in the present study, are shown in Table 1.

As seen from Fig. 3, the shape of the J_o–T–t curve obtained in the first heating-reduction run for t′($CeZrO_4$) was fairly complicated; two or three peaks appeared. Once the $CeZrO_4$ sample was reduced to pyrochlore and then oxidized at 873 K, the peak on the J_o–T–t curve of the second run became sharp and shifted toward the lowest temperature; this was attributable to the appearance of the metastable κ phase. As long as the redox cycle was continued without annealing in O_2 gas at 1323 or 1423 K, the shapes of the J_o–T–t curves of the second and third runs were fairly reproducible. Once the κ phase obtained by the oxidation at 873 K was annealed in O_2 gas at 1323 K, the J_o–T–t curve of the fourth run significantly shifted toward a higher temperature. When the pyrochlore phase obtained by this reduction was oxidized in O_2 at 873 K, the κ phase appeared again, and therefore the peak temperature, T_p, of the J_o–T–t curve for the fifth run became lower than that for the fourth run, though obviously higher than those of the second and third runs. Furthermore, as long as the redox cycle was continued without annealing in O_2 gas at 1323 or 1423 K, the shapes of the J_o–T–t curves were fairly reproducible. As the cyclic redox process proceeded, when the κ phase obtained by the oxidation at 873 K was annealed in O_2 gas at 1323 or 1423 K, the J_o–T–t curves of the seventh and tenth runs shifted toward the highest temperature and the peaks of the curves became very sharp. This was attributable to the appearance of the new t* phase.

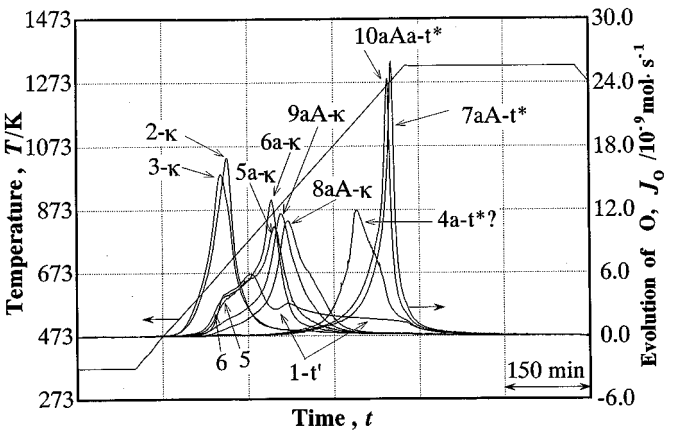

FIG. 3. J_o–T–t curves obtained in the heating-reduction runs, when the t′ phase was repeatedly reduced and then oxidized; the t′ was subjected to preliminary vacuum treatment ① at 1173 K for 1 h. J_o indicates the oxygen evolution rate in mol of O.The numerical value indicates the heating-reduction runnumber. "a" and "A" following the run number indicate the history of the sample annealed in O_2 gas at 1323 K and 1423 K, respectively.

TABLE 1
Lattice Parameters of t′ t*, κ and Pyrochlore Phases Obtained in the Present Study

Phase (composition)	Space group	Lattice parameter (nm)	Volume of unit cell (nm^3)
t′	tetragonal	$a = 0.52569(5)^{a,c}$	$V = 0.14662(3)$
($CeZrO_4$)		$b = 0.53055(4)^b$	$8V = 1.1723$
t*	tetragonal	$a = 0.52579(6)^a$	$V = 0.14669(4)$
($CeZrO_4$)		$b = 0.53062(7)$	$8V = 1.1735$
κ	cubic?	$a = 1.05332(2)^b$	$V = 1.16863(8)$
($CeZrO_4$)			
pyrochlore	cubic	$a = 1.07220(4)$	$V = 1.2326(1)$
($Ce_2Zr_2O_{7.016}$)	*Fd3m*		

[a] The lattice parameters of pseudofluorite cell.
[b] The symmetry may be lower than *Fd3m*, and may not be cubic; however, the lattice parameter was taken as twice that of CaF_2.
[c] The number in parentheses indicates estimated standard deviation of the last digit.

In Fig. 4, the powder XRD patterns of the phases ($CeZrO_4$) corresponding to the samples subjected to the first, third, seventh, and ninth heating-reduction runs are compared with that of the pyrochlore phase $\{Ce_2Zr_2O_{7+y}$ $(y = 0.016)\}$ obtained in the heating-reduction experiment. Fig. 4a shows the XRD pattern of the tetragonal t′ form. Cations, i.e., Ce and Zr atoms, in the t′ phase are randomly mixed; the (112) diffraction reflects the displacement of oxygen atoms along the *c*-axis, as reported by Yashima and Yoshimura (1). As seen in Figs. 4a and 4c, the powder XRD pattern of the t* phase for seventh run, which was obtained by annealing the κ phase in O_2 gas at 1423 K, was the same as that of t′. Figure 5 shows the Raman spectra for the t′ and t* phases. The shapes of the spectra resembled each other

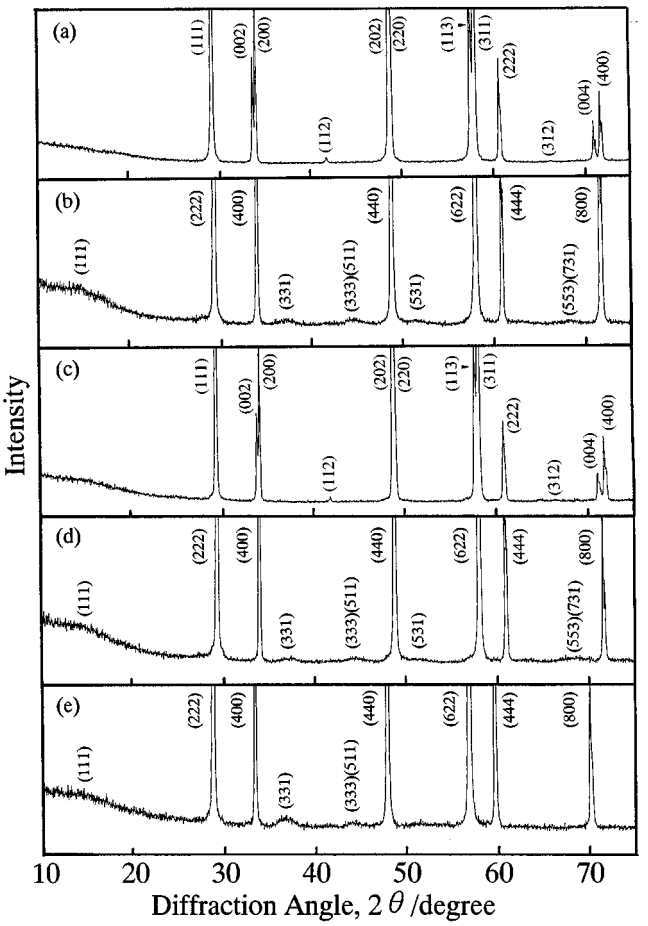

FIG. 4. The powder XRD patterns of the starting phases for the various heating runs, appearing in cyclic redox process, together with that of the pyrochlore phase.(a) 1-t′; (b) 3-κ; (c) 7aA-t*; (d) 9aA-κ; (e) pyrochlore, $\{Ce_2Zr_2O_{7+y}\,(y = 0.016)\}$. The number corresponds to the heating-reduction run number shown in Fig. 3. The symbols following the numbers indicate the type of identified phases.

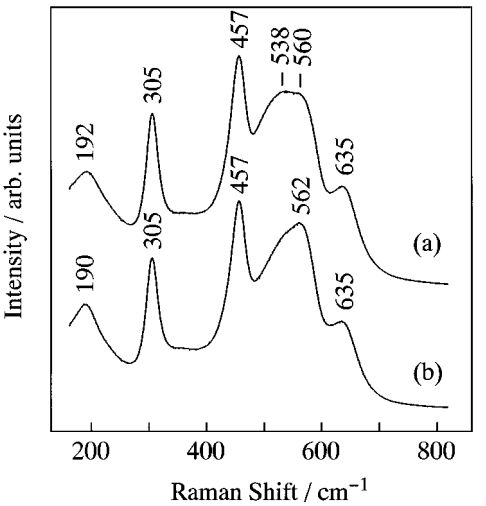

FIG. 5. Comparison of Raman spectra for t′ and t* phases. (a) t′, corresponding to the phase for heating-reduction run (1-t′) shown in Fig. 3; (b) t*, corresponding to the phase for heating-reduction run (7aA-t*) shown in Fig. 3.

very much; however, a small but clear difference in the relative peak strength for 538 and 562 cm^{-1} existed. The spectrum for the t′ was consistent with that reported previously (17). These results imply that the unit cells of t′ and t* were essentially the same. The random arrangement of Ce and Zr atoms and the displacement of oxygen atoms along the c-axis exist in the t* phase as in the t′ phase; however, there may still be some difference in the local displacement of oxygen atoms.

As seen in Figs. 4b, 4d, and 4e, the XRD patterns of the κ phases subjected to the third and ninth heating-reduction runs were very close to that of pyrochlore. Figure 6 shows the Raman spectra for the κ phases, which were completely different from those for pyrochlore. The Raman spectra for these κ phases, the oxygen release behaviors of which were different, resembled each other in appearance. However, the relative peak strengths, e.g., 274 and 306 cm^{-1} 570 and 603 cm^{-1} were clearly different, and further small peaks, e.g., 399 cm^{-1} appeared only in Fig. 6a. This result implies that there may be a difference in the local oxygen atom arrangements of the κ phases; the slight difference in the displacement led to varied oxygen release behavior of the κ phases.

Figures 7a and 7b show the J_o–T–t curves obtained when the starting phase of t′ was subjected to the preliminary vacuum treatment ②, that is, the system was not evacuated at a temperature as high as 1173 K. The shape of the J_o–T–t

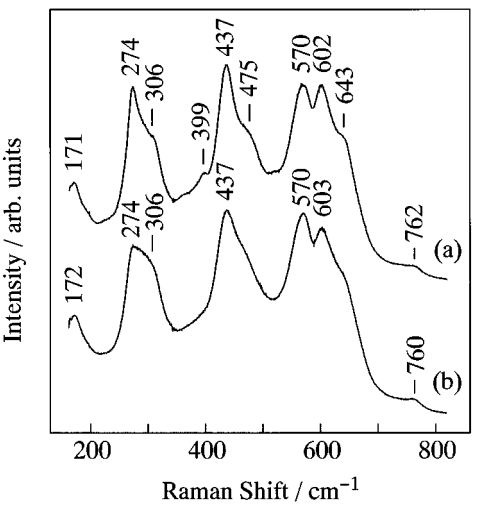

FIG. 6. Comparison of Raman spectra for κ phases. (a) κ phase corresponding to the phase for heating-reduction run (3-κ) shown in Fig. 3; (b), κ corresponding to the phase for heating-reduction run (9aA-κ) shown in Fig. 3.

curve for t′ in the first heating-reduction run was fairly simple, unlike that shown in Fig. 3. Furthermore, the peak on the J_o–T–t curves, e.g., for the fifth and sixth runs, was separated into two, i.e., around 723 K and 873 K. As the annealing of the κ phase in O_2 gas at 1323 or 1423 K was repeated, the J_o–T–t curves shifted toward the highest temperature. The trend in the change of the J_o–T–t curves with the run number was essentially the same as that observed in Fig. 3; however, the rate of the shift was smaller than that in Fig. 3, and therefore, the annealing time in O_2 gas at 1423 K after the tenth run was prolonged to 15 h. Eventually, the J_o–T–t curve in the eleventh run shifted to a high temperature, like that in the seventh run in Fig. 3. We carried out several series of experiments, but still could not conclude that differences in the shapes of the J_o–T–t curves and the appearance rate of t* with repeating heating-reduction run number could come from the difference in the preliminary vacuum treatment.

5. DISCUSSION

Very recently, the authors (10) measured the oxygen partial pressure over (t′, t*, or κ) + pyrochlore mixtures to evaluate the thermodynamic properties of these $CeZrO_4$ phases. It was found that a phase transition occurs between the two tetragonal phases, and the κ phase has the lowest thermodynamic stability. Assuming that the tetragonal phase thermodynamically more stable at lower temperatures than 1273 K was t*, the order of the thermodynamic stability became t*, t′, and κ in the intermediate temperature range (10). Thus, the results of the EGA analysis shown in Figs. 3 and 7 could be explained consistently in terms of thermodynamic stability. The onset and peak temperatures (around 523 and 673 K, respectively) of the J_o–T–t curves of the second and third runs for the κ phase, observed in the present study, were somewhat lower and the peak height was much higher than those for the κ phase made from (t + CeO_2) mixtures in the previous study (9). This may be attributed to the fact that the κ phase prepared in the present study was a single phase.

Although there was no difference among the XRD patterns of the κ phases and pyrochlore, one should recall that the pyrochlore as the precursor of the κ phase was made in the present study by annealing at 1323 K in a reducing gas. As seen in Fig. 4e, the diffraction peaks characteristic of the pyrochlore structure, e.g., (111), (331), (333), and (511), were small and broad; this phenomenon could be explained by the existence of an antiphase domain having a pyrochlore-type structure (18). Very recently, the authors (10, 19) have found that, when the pyrochlore was prepared at 1373 K, the diffraction peaks characteristic of the pyrochlore structure became stronger. The XRD pattern for the obtained κ phase was similar to that of the pyrochlore. Furthermore, additional peaks were observed which could be indexed on the basis of the lattice twice as large as CaF_2 structure; these diffractions, however, were forbidden, assuming a pyrochlore structure with space group *Fd3m*. The Raman spectra for the κ phases exhibited many peaks, unlike that for pyrochlore. These results imply that the κ phase may not belong to space group *Fd3m* due to displacement of oxygen atoms (18), although the cations take an ordered arrangement similar to pyrochlore. Detailed data on the characterization of the κ phases using XRD and Raman spectroscopy, which were obtained by changing widely the preparation temperature of the pyrochlore as the precursor, will be reported elsewhere (20).

A very important feature appearing in Figs. 3 and 7 is that various shapes of the J_o–T–t curves were obtained for the

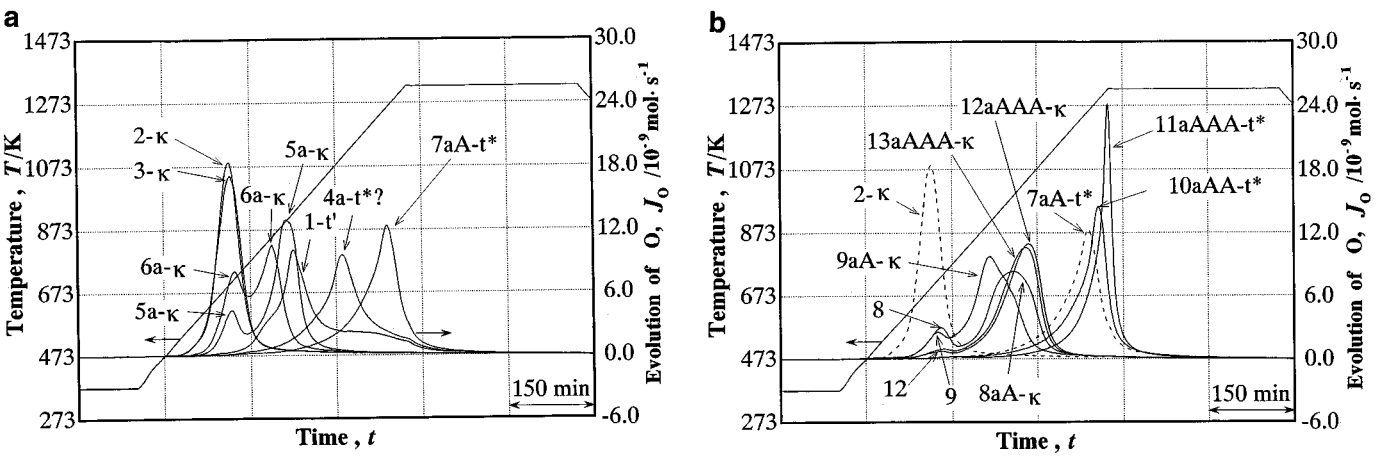

FIG. 7. J_o–T–t curves obtained in the heating-reduction runs, when the t′ phase was repeatedly reduced and then oxidized; the t′ phase was subjected to preliminary vacuum treatment ② at 373 K for 1 h. (a) runs 1–7; (b) runs 8–13. J_o indicates the oxygen evolution rate in mol of O. The numerical value indicates the heating-reduction run number. "a" and "A" following the run number indicate the history of the sample annealed in O_2 gas at 1323 K and 1423 K, respectively.

κ phases. The J_o–T–t curves shown in Fig. 3, for instance, were classified into three groups. The peak temperature, T_p, depended on whether the sample had experienced the t* phase; as the experience was longer, the T_p became higher. Furthermore, the cyclic redox process without annealing in O_2 at 1323 or 1423 K relaxed the effect of the history; for instance, the peak temperatures on J_o–T–t curves of the sixth and ninth runs in Fig. 3 became lower than those of the fifth and eighth runs, respectively. In the case of the fifth and sixth runs in Fig. 7, the peak around 723 K was increased, and the peak around 873 K shifted toward the lower temperature with decreasing strength.

As mentioned in the previous section, the displacement of oxygen atoms in the t* is slightly different from that in the t′; the t* possesses an inherent oxygen displacement. This displacement might affect the oxygen displacement in the κ phase obtained through the t* → pyrochlore → κ phase transitions. Thus, the effect of the t* on the displacement of oxygen atoms in the κ phase would disappear through the cyclic redox process between the pyrochlore and κ phases without the t*.

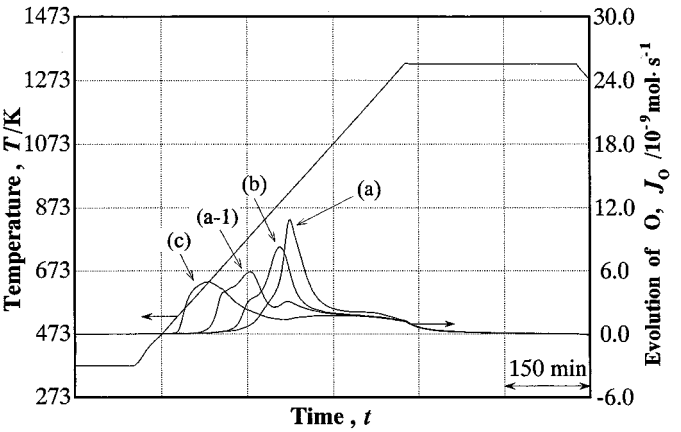

FIG. 8. J_o–T–t curves for t′ powders prepared by various procedures, where all the powders were oxidized in O_2 gas at 873 K for 5 h. (a) t′ as prepared, which was obtained by annealing the starting pellet in air at 1823 K for 50 h; (b) t′ obtained by annealing the pellet of sample a in air at 1823 K for 50 h; (c) t′ obtained by annealing the powders of sample b in air at 1823 K for 50 h; (a-1) the t′ powders of sample a were subjected to a preliminary vacuum treatmenta ① at 1173 K.

6. FURTHER EXPERIMENTS ON t′ AND DISCUSSION

The shape of the J_o–T–t curve of the first run in Fig. 3 was fairly complex; the starting t′ phase was subjected to a vacuum treatment and successive annealing in O_2 gas at 1173 K. We inferred that change in the chemical properties of t′ was induced by removing and then adding oxygen. The cubic phase at 1823 K, i.e., the precursor of the t′ phase, must involve a large amount of oxygen vacancies, because even air is a relatively reducing gas at an annealing temperature as high as 1823 K. In the cooling process, the phase becomes the t′ phase and then incorporates oxygen from the atmosphere; the rate of oxygen gained may depend on the morphology of the sample. Thus, we tried to compare the oxygen release behavior of three types of t′ powders. Sample a, the t′ single phase, was prepared by annealing the pellet of ZrO_2–CeO_2 mixtures at 1823 K for 50 h in air, as described in the previous section. Sample b was obtained by again annealing the pellet of sample a at 1823 K for 50 h in air. Sample b was crushed into a powder, and sample c was obtained by annealing the powder at 1823 K for 50 h in air. After the preliminary vacuum treatment ②, i.e., annealing at 1173 K in O_2 gas and successive evacuation at 373 K, the powders of samples a, b, and c were subjected to EGA analysis.

In Fig. 8, the EGA results for these powders are compared with that of the first run in Fig. 3; the latter result was designated as sample (a-1) in Fig. 8 because the starting sample corresponded to sample a with the preliminary vacuum treatment ① at 1173 K. As seen from Fig. 8. the shapes of the J_o–T–t curves and the peak temperatures, T_p, were significantly different. One may especially pay attention to the results for sample c, in which T_p was the lowest; sample c had been annealed three times at 1823 K, and therefore, its grain size might have become the largest..

Because sample c had been annealed as a powder at 1823 K, it might gain oxygen in air in the cooling process. If the temperature, T_g, where the sample incorporated a significant amount of oxygen from air or O_2 gas is considered, the temperature where sample c gained oxygen, $T_g(c)$, might be the highest, probably $T_g(c) > 1173$ K. In contrast, the pellets of samples a and b might gain only small amounts of oxygen during the cooling process from 1823 K. If this happens, the powders of samples a and b might gain oxygen during the heating process of preliminary treatment ② in O_2 gas from room temperature to 1173 K. Because the pellet of sample b had been annealed twice at 1823 K, its grain size might have become larger. Therefore, the $T_g(b)$ of the powder of sample b might be slightly higher than the $T_g(a)$ of the powder of sample a, for instance, $1173\text{ K} \gg T_g(b) > T_g(a)$. Because sample (a-1) was subjected to vacuum treatment and successive annealing in O_2 gas at 1173 K, $T_g(a\text{-}1) \approx 1173$ K held. Finally, we could infer a relation, $T_g(c) > 1173\text{ K} \approx T_g(a\text{-}1) \gg T_g(b) > T_g(a)$. For the peak temperatures in Fig. 8, a relation, $T_p(c) < T_p(a\text{-}1) < T_p(b) < T_p(a)$, held. Thus, the peak temperature, T_p, of the J_o–T–t curve for t′ appeared to be closely related to the temperature, T_g; T_p became lower with increasing T_g.

As seen in Fig. 8, two peaks on the J_o–T–t curve were observed for sample (a-1); T_p on the higher temperature side agreed with that for sample a. We could infer that the vacuum treatment of sample (a-1) at 1173 K undertaken for a few minutes could not affect oxygen in the inner part of particles; the chemical properties of sample a might be left there. Thus, difference in all the peak temperatures of the

J_o–T–t curves in Fig. 8 could be consistently explained in terms of the temperature, T_g, where oxygen was gained.

There was no difference among the XRD patterns of various t′ samples. Gaining oxygen did not affect the cation arrangement, but might induce a slight change in the displacement of oxygen atoms in the t′ phase. Generally, the t′ form has been studied as a single form; however, in view of various oxygen displacements in it, it may be of a generic form. In the case of the κ phase, a slight difference in the displacement of oxygen atoms led to the varied oxygen release behavior. The results for the t′ phase may be in line with those for the κ phase.

7. CONCLUSIONS

Evolved-oxygen gas analyses (EGA) were repeatedly carried out by heating t' in a reducing gas and successively oxidizing of the resulting pyrochlore phase in O_2 gas at various temperatures. The rate of oxygen released was analyzed as a function of temperature and time. The results obtained were as follows:

(1) The single κ phase ($CeZrO_4$) was obtained by oxidizing the pyrochlore phase at 873 K. When the κ phase was annealed in O_2 gas at 1323 or 1423 K, a new tetragonal phase t* appeared, which released oxygen at the highest temperatures.

(2) The κ phase may not belong to the space group $Fd3m$, although the XRD pattern is close to that of the pyrochlore.

(3) The onset and peak temperatures of oxygen release from the κ phase changed significantly and were dependent on whether the sample had experienced the t* phase.

(4) A difference among the κ phases exhibiting various oxygen release behaviors could not be detected by the powder XRD, but could by Raman spectroscopy.

(5) The oxygen release behavior of t′ significantly depended on the temperature where the t′ had gained oxygen after losing a small amount of oxygen; as this temperature increased, the onset temperature of oxygen release decreased.

(6) The t′ and t* phases could not be distinguished by the XRD technique; however, there was a slight difference in their Raman scattering spectra. This may imply a slight difference in the displacement of oxygen atoms in the t′ and t*.

ACKNOWLEDGMENTS

The authors are grateful to Dr. N. Umesaki and Professor N. Ohtori, who helped us use the Raman scattering apparatus at Osaka National Research Institute, AIST. We also thank Mitsui Metal Co., Ltd., for the supply of CeO_2 and ZrO_2 powders and H. Miyagishi for his experimental assistance. The authors are grateful for support by Grant-in-Aid for General Scientific Research 08875139 from the Ministry of Education, Science and Culture, Japan.

REFERENCES

1. M. Yashima and M. Yoshimura, *Materia Japan* **34,** 448 (1995).
2. M. Yashima, H. Takashima, M.Kakihana, and M. Yoshimura, *J. Am. Ceram. Soc.* **77,** 1869 (1993).
3. T. Muroi, J. Echigoya, and H. Suto, *Trans. Jpn. Inst. Met.* **29,** 634 (1988).
4. M. Yashima, K. Morimoto, N. Ishizawa, and M. Yoshimura, *J. Am. Ceram. Soc.* **76,** 2865 (1993).
5. S. Matsumoto, *Toyota Technical Review* **44,** 12 (1994).
6. S. Matsumoto, N. Miyoshi, T. Kanazawa, M. Kimura and M. Ozawa, *Catalytic Sci. Technology* **1,** 335 (1991).
7. M. Ozawa, M. Kimura, and A. Isogai, *J. Alloys Compd.* **193,** 73 (1993).
8. T. Murota, T. Hasegawa, S. Aozasa, H. Matsui, and M. Motoyama, *J. Alloys Compd.* **193,** 298 (1993).
9. S. Otsuka-Yao, H. Morikawa, N. Izu, and K. Okuda, *J. Japan Inst Metals* **59,** 1237 (1995).
10. S. Otsuka-Yao-Matsuo, N. Izu, T. Omata, and H. Ikeda, *J. Electrochem. Soc.* **145,** 1406 (1998).
11. M. Yu. Sinev, G. W. Graham, L. P. Haack, and M. Shelf, *J. Mater. Res.* **11,** 1960 (1996).
12. S. Yao, H. Uchida, and Z. Kozuka, *Mater. Trans., JIM.* **31,** 999 (1990).
13. S. Otsuka and Z. Kozuka, *Trans. Jpn. Inst. Met.* **25,** 639 (1984).
14. S. Otsuka and Z. Kozuka, *Metall. Trans. B* **16,** 113 (1985).
15. K. Kiukkola and C. Wagner, *J. Electrochem. Soc.* **104,** 379 (1957).
16. S. Yao, H. Tanaka, and Z. Kozuka, *J. Jpn. Inst. Met.* **55,** 1216 (1991).
17. M. Yashima, H. Arashi, M. Kakihara, and M. Yoshimura, *J. Am. Ceram. Soc.* **77,** 1067 (1994)
18. T. Moriga, S. Emura, A. Yoshiasa, S. Kikkawa, F. Kanamaru, and K. Koto, *Solid State Ionics* **40/41,** 357 (1990).
19. H. Kishimoto, T. Omata, S. Otsuka-Yao-Matsuo, N. Otori, and N. Umesaki, *in* "Abst. of Annual Meeting of Jpn. Inst. Met.," p. 333, Tokyo, Japan, March, 1997.
20. T. Omata, H. Kishimoto, and S. Otsuka-Yao-Matsuo, Unpublished research, Osaka University, 1997.